Impact Assessment and Mitigation Techniques for High Penetration Levels of Renewable Energy Sources in Distribution Networks: Voltage-control Perspective

Ahmed S. A. Awad, Dave Turcotte, and Tarek H. M. El-Fouly

***Abstract*—The integration of renewable distributed generation (RDG) into distribution networks is promising and increasing nowadays. However, high penetration levels of distributed generation (DG) are often limited as they may have an adverse effect on the operation of distribution networks. One of the operation challenges is the interaction between DG and voltage-control equipment, e. g., an under-load tap changer (ULTC), which is basically designed to compensate for voltage changes caused by slow load variations. The integration of variable DGs leads to rapid voltage fluctuations, which can negatively affect the tap operation of ULTC. This paper investigates the impact of high penetration levels of RDG on the tap operation of ULTC in distribution networks through simulations. Various mitigation techniques that can alleviate this impact are also examined. Among these techniques, constant power-factor mode is regarded as the best trade-off between the simplicity and effectiveness of minimizing the number of tap operations. Simulations are performed on a Canadian benchmark rural distribution feeder using OpenDSS software.**

***Index Terms*—Renewable energy, distributed generation (DG), voltage regulator, load tap changer, distribution network.**

I. Introduction

THE potential for the large-scale integration of distributed generation (DG), especially renewable DG (RDG), is promising and continuously increasing. DG has numerous benefits to distribution networks, e. g., enhancing reliability, supporting voltage regulation, and reducing energy losses. For instance, a method was proposed in [1] for allocating (i.e., siting and sizing) DG units in distribution networks to minimize the investments of network upgrade and costs of energy losses; and to enhance the network reliability. In [2], solar-based DG was used to minimize a voltage-deviation index through full utilization of DG capabilities via enabling reactive power exchange with the power grid, i. e., injecting or absorbing reactive power.

Distribution networks have traditionally been equipped with the devices to control the voltage profiles, e.g., load tap changers and capacitor banks. The high penetration levels of DG can negatively affect the operation of these voltage-control devices. The work proposed in [3] discussed the impact of DG on the voltage control in distribution networks, but without quantifying such impact through performing simulations on typical distribution networks. In [4] and [5], the impact of solar-based DG on the voltage regulation and system protection was evaluated. Some mitigation techniques such as constant power factor (PF) or dynamic voltage control (e. g., volt-var control) were further suggested to mitigate voltage-related problems. However, the case studies did not consider various locations and sizes of DG units. As such, the conclusions were neither comprehensive nor showing the locational effects of DG integration. A simulation-based study was conducted in [6] to determine the impact of high penetration levels of photovoltaic (PV) on the voltage profiles in distribution networks. It was concluded that the voltage profiles were not adversely affected when the PV ratings did not exceed 2.5 kW per household on average in a typical distribution network. In [7], a study was proposed to investigate the impact of high penetration levels of PV on several matters, i.e., active power losses, peak load, reverse power flow, voltage excursions, and tap operation of voltage regulators. Eight representative feeders and three different locations were used in the latter study. It was inferred that the feeder location had a stronger impact than the feeder type on the incidence of reverse power flow and presence of voltage excursions. On the other hand, feeder characteristics were found to be the dominant factor in regards to the number of tap operations. The PV penetration was randomly distributed among available houses in each distribution feeder; there-

Manuscript received: March 21, 2020; revised: July 8, 2020; accepted: September 3, 2020. Date of CrossCheck: September 3, 2020. Date of online publication: April 5, 2021.

The authors would like to thank the Government of Canada for financially supporting this research through the Program on Energy Research and Development (PERD), the Wind Energy Institute of Canada (WEICan) for providing the data of its 10 MW wind farm required in this paper, and Daniel Desrosiers and Ali Mehrizi-Sani for their helpful comments and suggestions.

A. S. A. Awad (corresponding author) is with Natural Resources Canada, CanmetENERGY, Varennes, Canada, on leave from the Electrical Power and Machines Department, Faculty of Engineering, Ain Shams University, Cairo 11566, Egypt (e-mail: ahmed.awad@canada.ca).

D. Turcotte is with Natural Resources Canada, CanmetENERGY, Varennes, Canada (e-mail: dave.turcotte@canada.ca).

T. H. M. El-Fouly is with Advanced Power and Energy Center, Khalifa University, Abu Dhabi, United Arab Emirates (e-mail: tarek.elfouly@ku.ac.ae).

DOI: 10.35833/MPCE.2020.000177

fore, the locational effects of PV were not methodically investigated.

The coordination between DG and conventional voltage-control equipment has also attracted the interests of many researchers. In [8], a voltage coordination scheme was introduced for allowing DG and other devices (capacitor banks, energy storage, etc.) to support passive means, i. e., underload tap changer (ULTC), in controlling the voltage profile of distribution feeders. A method was proposed in [9] to determine the optimal PF and tap settings for DG and ULTC, respectively, to allow for the integration of higher capacities of DG while satisfying the voltage limits of the distribution networks. In [10], a coordinated voltage-control algorithm was proposed to harmonize the control actions of ULTC and DG units. A vehicle-to-grid reactive power support strategy was introduced in [11] for optimizing the coordinated voltage regulation in distribution networks with high penetration levels of DG and plug-in electric vehicles. References [12], [13] developed data-driven frameworks for controlling the power injections from distributed energy resources (DERs) and tap settings of ULTCs in distribution networks with the objective of regulating voltages. In [14], a novel two-timescale voltage regulation scheme was developed for controlling smart inverters and shunt capacitors in distribution networks using data-driven and physics-based optimization.

From the aforementioned literature, some researches evaluated the impact of RDG on the tap operation of ULTC. However, the locational effect and impact of different penetration levels of DG were not systematically studied. Other researches also developed techniques to alleviate some of the negative impacts of high penetration levels of DG through optimizing the control actions or settings of DG and ULTC. However, a fair comparison of various techniques in mitigating the impact of high penetration levels of DG was not conducted. To fill these gaps and provide practical insights, the contributions of this paper are as follows.

1) The impact of the location and penetration level of RDG on the operation of ULTC is investigated through performing various simulations on a benchmark distribution network.

2) Theoretical analysis and technical discussions are provided to support the numerical results obtained.

3) The most effective mitigation techniques are examined and identified for reducing the operation number of ULTC with high penetration levels of RDG.

The remainder of this paper is organized as follows. In Section II, the system under study and simulation data are proposed. The impact assessment and mitigation techniques are then discussed in Sections III and IV, respectively. Finally, Section V summarizes the conclusions of the research performed in this paper.

II. Case Study

A. System Description

The data of the Canadian benchmark rural distribution network used in this study are taken from [15]. It consists of a radial distribution feeder as shown in Fig. 1. The transformers T1, T3, and T4 are three-phase and medium-voltage transformers. The regulating transformer T2 is equipped with a ULTC on the secondary winding with ±10% voltage variation over 32 steps. Two strategies are considered for controlling the ULTC as follows.

1) A fixed voltage at the feeder end is maintained using line-drop compensator (LDC).

2) A fixed voltage at the terminals of the regulating transformer is maintained without LDC.

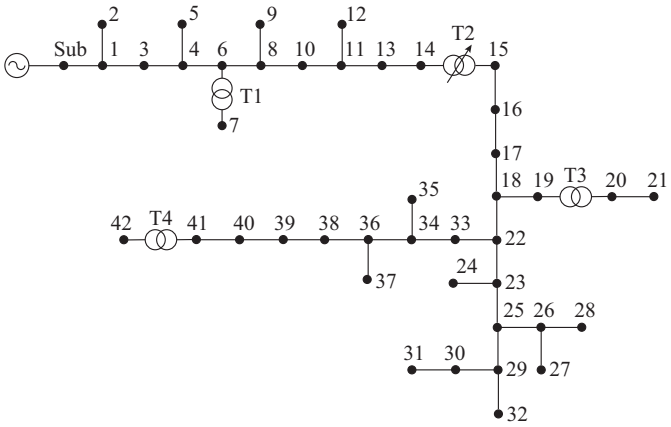

Fig. 1. Topology of Canadian benchmark rural distribution network.

The voltage set points for both strategies are 1 p.u. with control bandwidth of 1.67%. The loads are assumed to operate at a constant PF of 0.9 (inductive), and their respective rated power values are summarized in Table I. This network is modelled using OpenDSS, an open-source distribution network simulator developed by Electric Power Research Institute (EPRI) [16].

TABLE I
Load Data of Rural Distribution Feeder

Number of node	Rated power (kVA)	Number of node	Rated power (kVA)
3	2370	24	50
5	400	28	160
7	3400	31	200
9	250	32	470
12	10	35	200
13	280	37	100
21	650	38	150
22	10	42	2300

Regarding the parameters of the LDC, the two-point method [17] is used to determine the resistance R_{line} and reactance X_{line} of the distribution feeder between the voltage regulator and the furthest load point. The furthest load point refers to the last point in the feeder that experiences the most voltage drop, which is node 41 in this case study. Applying the two-point method yields 2.2 Ω and 4.2 Ω for R_{line} and X_{line}, respectively, which are calculated at the main feeder side.

B. Data Processing

The data used in this study include actual measurements

from PV and wind farms in addition to a typical load profile. This subsection introduces the sources of these data and the methodology adopted to process them before performing the main analysis.

1) Renewable Resources

The data of renewable resources are taken from two systems: a simulated PV farm in Varennes, QC, Canada, and a 10 MW wind farm in North Cape, PEI, Canada, in 2015 and 2016. The data of both systems are available at 1-minute intervals. The power data of the wind farm are actual data, while the power data of the PV farm are estimated since it is a virtual PV farm.

The output power of the PV farm in Varennes is estimated using actual measurements of solar radiation collected from 17 high-resolution irradiance sensors [18]. The irradiance data of a single sensor are smoothed to represent the average irradiance over the PV farm using the wavelet variability model developed by Sandia National Laboratories [19]. This model needs several parameters for the PV farm as inputs, including the farm capacity, PV farm density (assumed to be 41 W/m^2, as in [19]), and average daily cloud speed. The average cloud speed is estimated from the data of multiple sensors using the cross-correlation algorithm described in [20]. The output power of the PV farm P_{PV} is estimated by:

$$P_{PV}=N_m P_{mp}(G,T_c) \tag{1}$$

$$P_{mp}(G,T_c)=\min\left(\frac{G}{1000},1\right)P_{\max}[1-TC_P\cdot(25-T_c(G))] \tag{2}$$

$$T_c(G)=T_a+\frac{NT-20}{800}G \tag{3}$$

where N_m is the number of modules; $P_{mp}(G,T_c)$ is the function of the maximum available power, G is the solar irradiance, T_c is the cell temperature; $P_{\max}$ is the rated power of a single PV module; TC_P is the temperature coefficient of the maximum power; T_a is the ambient temperature; and NT is the normal cell temperature estimated at an ambient temperature of 20 ℃ and irradiance level of 800 W/m^2 [21].

The parameters of the 280 W PV module are obtained from the data sheet of the manufacturer [22]. The number of modules N_m is varied to obtain the required capacity of PV farm. The data of solar irradiance are collected in 2015 and 2016. The ambient temperatures during this period are further obtained from Environment and Climate Change Canada [23].

For the purpose of comparing the variability in PV and wind farms, the PV farm is assumed to have the same power capacity as the wind farm, i.e., 10 MW. The daily power profiles of both PV and wind farms are normalized and characterized based on the curve length as a measurement of the variability. All days are then sorted according to the curve length, and the first quartile of days with the most variable data (i.e., longest curve lengths) is identified. Table II summarizes the minimum, median, and maximum curve lengths of the most variable data for both systems. Sample days, corresponding to the days with the minimum curve lengths, are also given in Table II. The power generation profiles on these days are shown in Figs. 2 and 3, respectively.

TABLE II
STATISTICS AND SAMPLE DAYS OF HIGHLY VARIABLE DATA

System	Curve length of highly variable data (p.u.·h)			Sample day
	Minimum	Median	Maximum	
PV farm	34.02	42.03	64.61	May 26, 2016
Wind farm	42.68	49.36	78.09	June 3, 2016

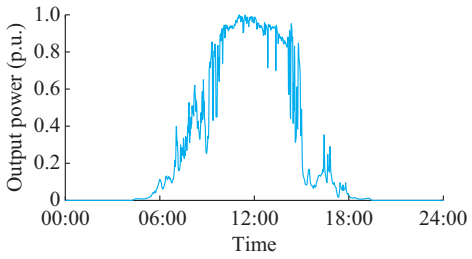

Fig. 2. Highly variable PV generation on May 26, 2016.

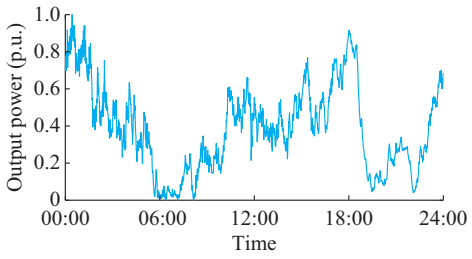

Fig. 3. Highly variable wind power generation on June 3, 2016.

2) Load Profile

The demand profile at each node is assumed to follow the IEEE-RTS load profiles in [24], which provide the hourly load magnitude normalized to the peak demand.

3) Data Preparation

The data introduced in the previous subsections have various resolutions ranging from one minute to one hour. Assuming that ULTC will take tap decisions every minute, given that the mechanical and control time delays are typically less than 1 min [11], the required resolution for the analysis is set at 1 min. Low-resolution data, i.e., 1 hour, of the load profiles are interpolated using the cubic spline function in MATLAB to generate data at one-minute intervals.

4) Voltage Limit

Standard CAN3-C235-83 specifies the normal and emergency voltage limits for the feeders up to 50 kV [25]. Under normal operation conditions, the voltage at service entrances (120 V or 240 V) should be kept between 0.917 p.u. and 1.042 p.u., while under extreme conditions, the voltage limits are 0.883 p.u. and 1.058 p.u.. At the feeder level, between 1 kV and 50 kV, the maximum recommended voltage deviation is ±6%, which is adopted in this study.

III. IMPACT OF RDG ON OPERATION OF ULTC

In this section, the impacts of wind- and solar-based DGs on the operation of LDC-based and conventional ULTCs are investigated at three different locations (nodes), namely, node 41 close to the feeder end, node 16 close to the voltage

regulator, and node 1 close to the feeder starting point. The profiles of sample days for PV and wind farms as well as the summer load of IEEE RTS, introduced in Section II-B, are used in this case study. In all cases, the DG is assumed to operate at unity PF.

A. Solar-based DG

Figures 4 and 5 show the tap locations for the base case (i.e., without DG) and the cases of 10 MW solar-based DG at three different locations with LDC-based and conventional ULTCs, respectively. It is clear that the LDC-based ULTC leads to more tap operations compared with conventional ULTC at the same DG penetration level and location. This can be attributed to the fact that LDC-based controller makes a decision based on estimating the feeder-end voltage using the Kirchhoff's voltage law in (4), as opposed to the conventional ULTC that controls the voltage based on actual measurements. Thus, the estimation-based control used by the LDC circuit could lead to a disturbance in the system voltages and the tap locations with the high penetration levels of DG.

$$V_L = V_R - I(R_{line} + \mathrm{j}X_{line}) \tag{4}$$

where V_R and V_L are the voltages at the regulator and furthest load point, respectively; and I is the line net-load current.

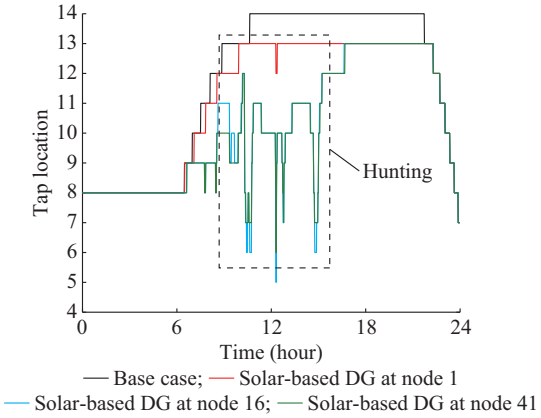

Fig. 4. Tap locations for base case and 10 MW solar-based DG at different locations with LDC-based ULTC.

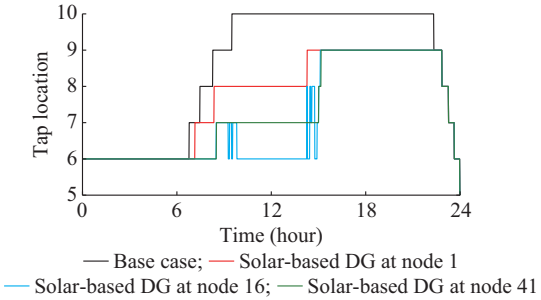

Fig. 5. Tap locations for base case and 10 MW solar-based DG at different locations with conventional ULTC.

Also, in Figs. 4 and 5, the hunting problem is noticed with both types of ULTC around noon time, i.e., peak time of the production for solar-based DG, especially with LDC-based ULTC and DG at nodes 16 and 41. The hunting problem is a phenomenon that infers an excessive number of tap operations (fluctuations), which occurs due to the quick variations in the power injected from DG. This problem is not favourable from the ULTC perspective.

Considering the impact of DG location, DG concentration close to the ULTC (node 16) is the worst case, followed by the cases of DG close to the feeder end (node 41) and feeder starting point (node 1). This can be explained by the fact that the regulator voltage and feeder-end voltage calculated using the LDC circuit are the highest when DG is close to the ULTC. Therefore, with DG concentration closer to the ULTC, more tap operations are required to bring the controlled voltage back to the desired range.

B. Wind-based DG

The tap locations for the base case (i.e., without DG) and the cases of 10 MW wind-based DG at different locations with LDC-based and conventional ULTCs are shown in Figs. 6 and 7, respectively. Similar to the solar-based DG cases, the number of tap operations depends on the location of DG; the worst case occurs when the DG concentration is located close to the ULTC.

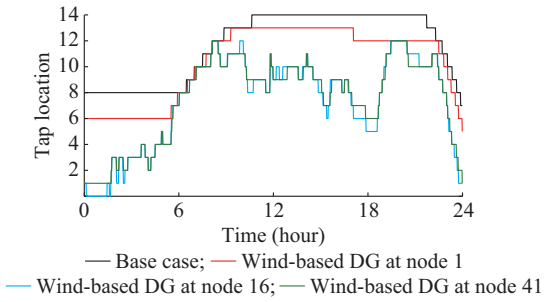

Fig. 6. Tap locations for base case and 10 MW wind-based DG at different locations with LDC-based ULTC.

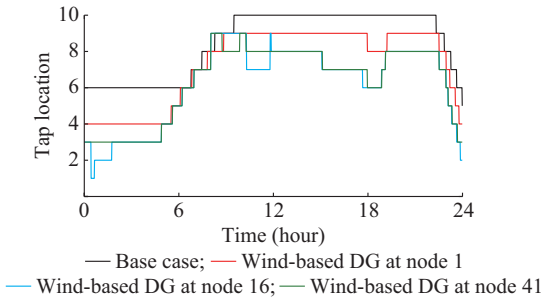

Fig. 7. Tap locations for base case and 10 MW wind-based DG at different locations with conventional ULTC.

The impacts of high penetration levels of DG on the voltages of regulated node 15 and node 41 with conventional and LDC-based ULTCs are illustrated in Figs. 8 and 9, respectively. These figures show the time-varying voltages for the base case and case of 10 MW wind-based DG located at node 16 as an example. It can be observed that the conventional ULTC successfully maintains the regulated voltage of node 15 within the regulating range (1±0.0083 p.u.) even in the worst-case scenario, i.e., the high penetration level of DG located at node 16. On the other hand, the LDC-based

ULTC does not maintain the regulated voltage of node 41 within the same regulating range at the same penetration level and location. This anomaly is due to the fact that the LDC-based ULTC is deceived by the injected current from DG, which reduces the net load current in the LDC circuit. Consequently, the LDC-based ULTC lowers its tap location assuming that the load is reduced, thus resulting in lesser voltages than at the lower bandwidth level. Nevertheless, from Figs. 8 and 9, it is depicted that all voltages are kept within the normal voltage limits (1±0.06 p.u.) with conventional and LDC-based ULTCs, which are the ultimate criteria for power quality.

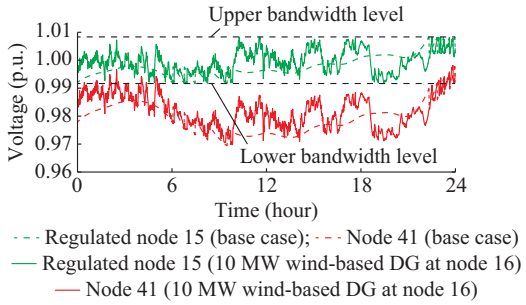

Fig. 8. Voltage profiles with conventional UTLC.

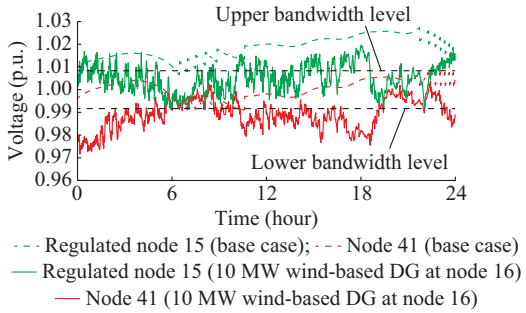

Fig. 9. Voltage profiles with LDC-based UTLC.

C. Summary of Results

Figures 10 and 11 compare the number of daily tap operations for all cases. As depicted, the LDC-based ULTC results in a larger number of tap operations compared with the conventional ULTC, especially with 10 MW wind-based DG located at node 16, where 84 and 18 tap operations are observed for LDC-based and conventional ULTCs, respectively. The number of tap operations also increases with larger penetration levels of DG, where 13 and 84 tap operations are depicted for the base case and case of 10 MW wind-based DG at node 16 with LDC-based ULTC.

IV. Mitigation Techniques for Reducing Number of Tap Operation

In the previous section, the impact of variability of RDG on the tap operation of ULTC is studied. It is concluded that large capacities of solar- and wind-based DGs generally lead to an excessive number of tap operations. This section proposes possible solutions that can reduce these tap operations with high penetration levels of renewable energy.

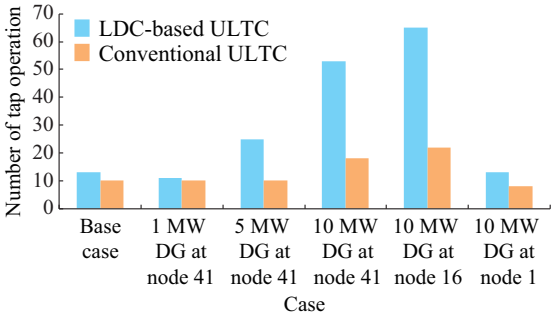

Fig. 10. Number of daily tap operations for base case and several cases of solar-based DG.

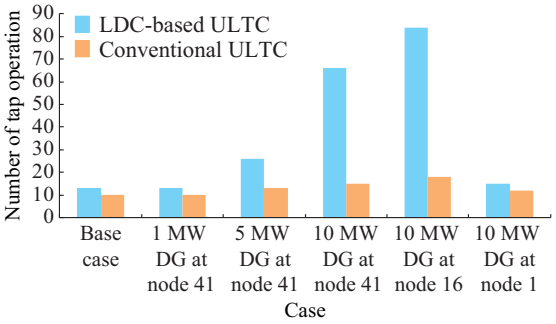

Fig. 11. Number of daily tap operations for base case and several cases of wind-based DG.

The proposed solutions include modified ULTC controller and voltage-reactive power (volt-var) control. According to IEEE Std. 1547-2018 [26], the DG can provide voltage regulation through changing the reactive power with any of the following functions: constant PF, volt-var, active power-reactive power, and constant reactive power. Each of these functions can be activated one at a time. Among these functions, constant PF and volt-var control are considered in this section. All of the proposed solutions are compared with the base case, which assumes unity PF for the DG and conventional ULTC controller.

A. Modified ULTC Controller

As opposed to conventional and LDC-based ULTCs discussed in Section II, the modified ULTC controller proposed in this section relies on estimating the maximum and minimum voltage downstream of the ULTC ($V_{\max}$ and $V_{\min}$) [11]. The control diagrams of conventional and modified ULTC controllers are shown in Fig. 12. The primary controller consists of dead zone, time delay, and motor drive, as in [11]. The modified ULTC controller takes an action to increase or reduce its tap location Δtap if these minimum or maximum voltages exceed the lower or upper voltage limits (V_{lower} and V_{upper}), respectively. The results of the base case, i.e., conventional and modified ULTC controller, are shown in Figs. 13 and 14 for 10 MW of solar-based DG at node 16. It can be seen that the taps of ULTC (under modified controller) do not change and keep the same location over the whole day while satisfying the upper and lower voltage limits. However, the drawbacks of this modified ULTC controller are as follows.

1) It is a complex solution as it requires a state estimation algorithm to evaluate the maximum and minimum voltages of the network.

2) The hunting problem could happen if overvoltage and undervoltage occur simultaneously in the network as reported in [11].

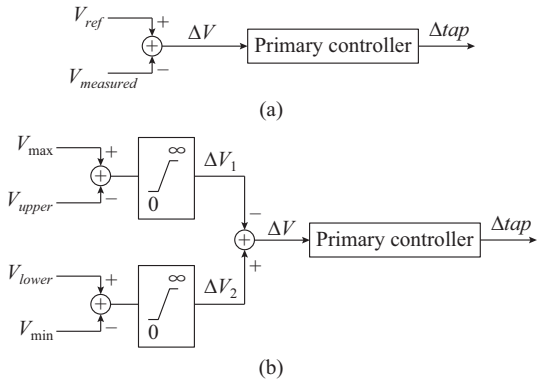

Fig. 12. Control diagram of different ULTCs. (a) Conventional ULTC. (b) Modified ULTC.

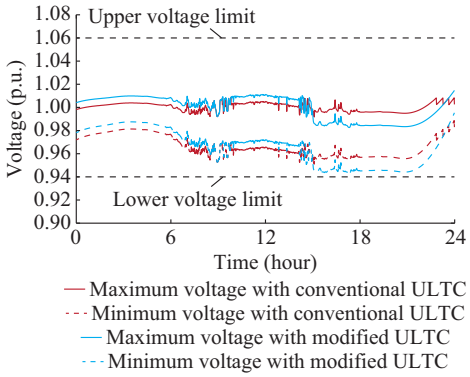

Fig. 13. Maximum and minimum network voltages with conventional and modified ULTCs.

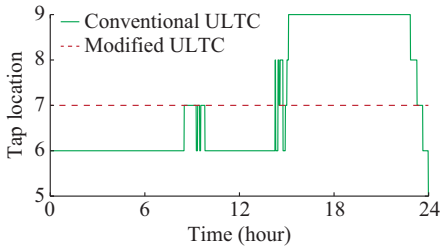

Fig. 14. Tap locations with conventional and modified ULTCs.

B. Constant PF Mode

Through allowing DG to consume or supply reactive power, the overvoltage and undervoltage problems can be solved without advanced algorithms. Under constant PF, the DG will consume or supply a certain amount of reactive power that is proportional to the active power generated at any time. As shown in Figs. 15-18, the results for the 10 MW solar-based DG at nodes 16 and 41 are compared with the base case, i.e., unity PF, and the case with constant PF of 0.99 (leading), i.e., absorbing reactive power. As depicted in the case of DG at node 16, the tap operations are significantly reduced from 23 to 7 per day (with the base case), as shown in Fig. 16. This reduction is due to regulating the voltage of DG through absorbing reactive power, thus leading to less interactions from the ULTC. With DG at node 41, tap locations are found to be the same as the base case (i.e., 7 tap operations per day), but with a better voltage regulation (i.e., closer to 1 p.u.), as shown in Figs. 17 and 18. However, choosing the value for constant PF can be critical and network or location dependent. For instance, with PF of 0.95 (leading) at nodes 16 and 41, the number of tap locations increases compared with that of the base case, and the hunting effect takes place with DG at node 41, as shown in Figs. 19 and 20. These issues occur because the DG units with high reactive power compensation tend to drag the network voltages below the normal range (i.e., 1 p.u.), and thus the ULTC is required to compensate these low voltages via increasing the tap location.

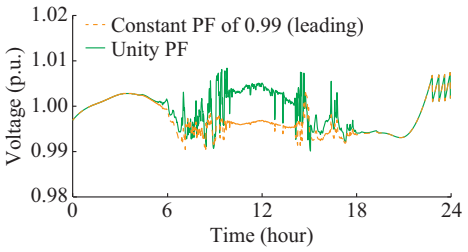

Fig. 15. Voltage of DG at node 16 with unity PF and constant PF of 0.99.

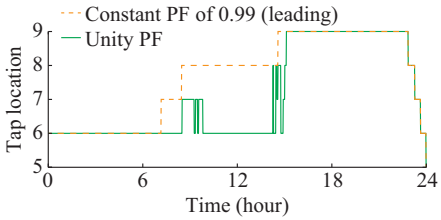

Fig. 16. Tap location with DG at node 16 with unity PF and constant PF of 0.99.

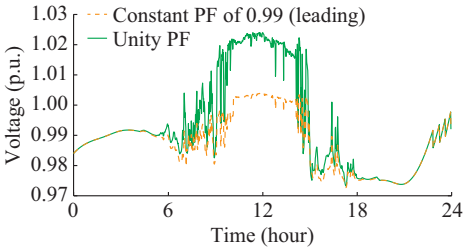

Fig. 17. Voltage of DG at node 41 with unity PF and constant PF of 0.99.

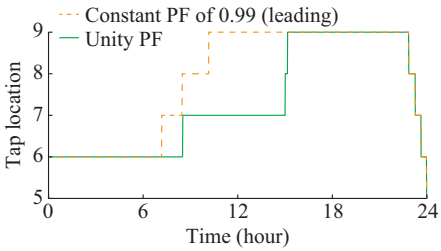

Fig. 18. Tap location with DG at node 41 with unity PF and constant PF of 0.99.

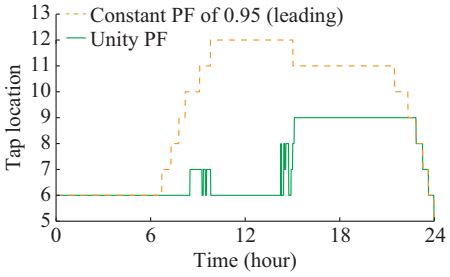

Fig. 19. Tap location with DG at node 16 with unity PF and constant PF of 0.95.

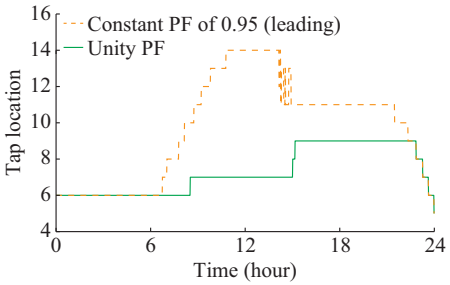

Fig. 20. Tap location with DG at node 41 with unity PF and constant PF of 0.95.

C. Volt-var Control

Similar to constant PF mode, volt-var control can compensate for voltage variations at the DG terminals. The typical characteristics of volt-var control are illustrated in Fig. 21. These characteristics imply that the DG is required to inject or absorb a certain amount of reactive power if the voltage at its terminals is lower or higher than a certain threshold, respectively. To implement this control methodology, an interface is established between MATLAB and OpenDSS. The control circuit is developed in MATLAB, and the reactive power signal is sent to OpenDSS for simulating the distribution network and returning the voltages of DG terminals to MATLAB. The flowchart of volt-var control developed in MATLAB is shown in Fig. 22. The main step in this control is to ensure that the slope of the linear part of volt-var characteristics (VVCs) is less than the change of reactive power with respect to the change in voltage. Too steep volt-var curves can lead to oscillations between two points in two different regions of the VVCs. In such cases, the reactive power required must be gradually reduced until it fulfills the VVCs of the distribution network.

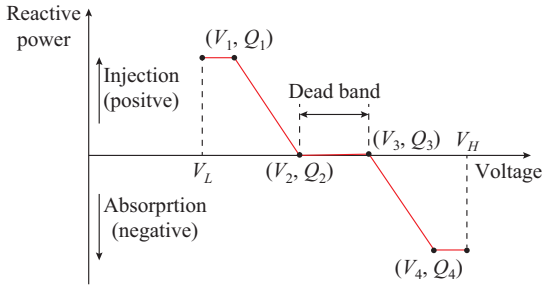

Fig. 21. Typical characteristics of volt-var control.

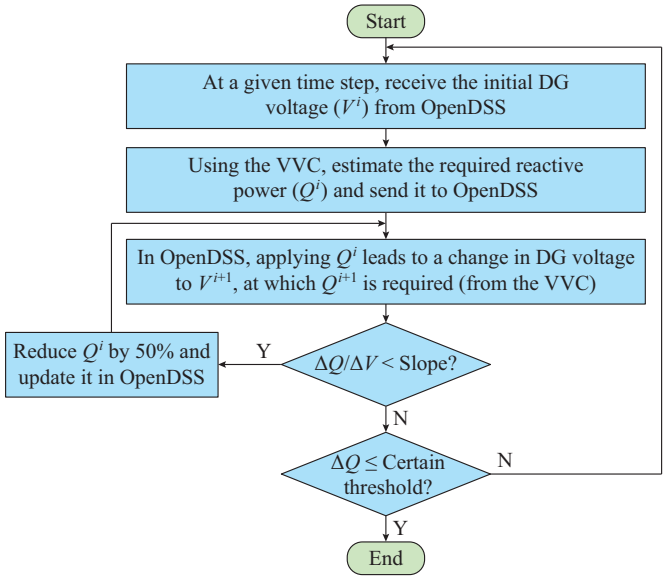

Fig. 22. Flowchart of volt-var control.

The results of the base case and volt-var control are compared with 10 MW solar-based DG at nodes 16 and 41. Regarding the volt-var control settings, the default settings as per IEEE Std. 1547-2018 are proposed in Table III. With these default settings, the dead-band region is between 0.98 p.u. and 1.02 p.u., which contains almost all the voltages of DG terminals, as shown in the base cases in Figs. 23 and 24. Then, if these default settings are applied to this network, very little or no reactive power will be consumed, and thus the volt-var control will be useless. Therefore, the voltage settings are modified, as shown in Table III, within the range of allowable settings suggested by the same standard. As shown in Fig. 25, the number of daily tap operations is reduced by 15 with the volt-var control at node 16. On the other hand, the number of tap operations does not change with volt-var control at node 41 in Fig. 26, but the voltage regulation is slightly enhanced.

TABLE III
VOLT-VAR CONTROL SETTINGS

Setting	V_1 (p.u.)	V_2 (p.u.)	V_3 (p.u.)	V_4 (p.u.)	Q_1/Q_4^* (%)	Q_2/Q_3^* (%)
Default setting	0.92	0.98	1.02	1.08	44	0
Modified setting	0.91	0.97	1.00	1.06	44	0

Note: * represents the percentage of apparent power rating.

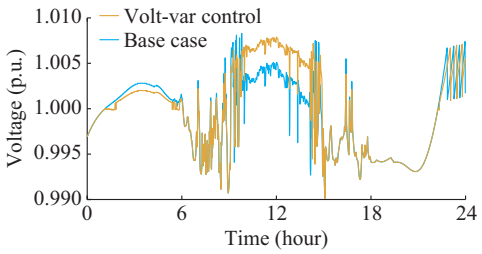

Fig. 23. Voltage of DG at node 16 with base case and volt-var control.

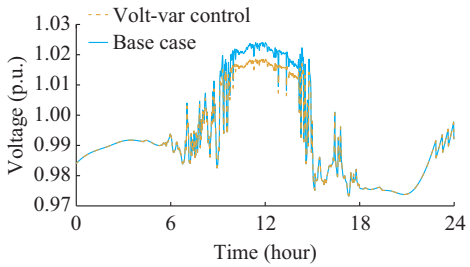

Fig. 24. Voltage of DG at node 41 with base case and volt-var control.

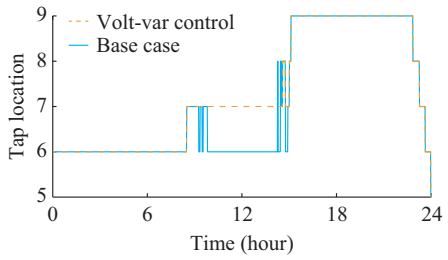

Fig. 25. Tap locations with DG at node 16 with base case and volt-var control.

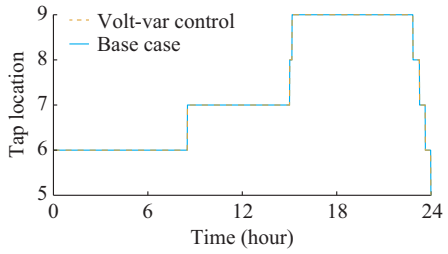

Fig. 26. Tap locations with DG at node 41 with base case and volt-var control.

V. Conclusion

This paper investigates the impact of integrating high penetration levels of RDG (operating at unity PF) on the tap operation of ULTC in Canadian typical rural distribution networks. It is generally concluded that the number of tap operations is less with conventional ULTC than that with LDC-based ULTC and with the same penetration level and location of DG. Regarding the locational effects, DG concentrations close to the secondary terminals of ULTC are found to be the worst case, followed by the cases of DG close to the feeder end and feeder starting point. Moreover, the results with LDC-based ULTC show that high penetration levels of DG could affect the capability of ULTC to keep the voltage of the feeder end within the desired range, i.e., control bandwidth, but within the normal voltage limits.

Various techniques are also investigated for reducing the number of tap operations with RDG. These techniques include modified ULTC controller, constant PF mode, and volt-var control. Among these techniques, modified ULTC controller is the most effective but most complex solution as it relies on estimating the maximum and minimum voltages of the network. On the other hand, constant PF mode seems to be the best trade-off between simplicity and effectiveness.

References

[1] M. F. Shaaban, Y. M. Atwa, and E. F. El-Saadany, "DG allocation for benefit maximization in distribution networks," *IEEE Transactions on Power Systems*, vol. 28, no. 2, pp. 639-649, May 2013.

[2] M. Ammar and A. M. Sharaf, "Optimized use of PV distributed generation in voltage regulation: a probabilistic formulation," *IEEE Transactions on Industrial Informatics*, vol. 15, no. 1, pp. 247-256, Jan. 2019.

[3] R. O'Gorman and M. Redfern, "The impact of distributed generation on voltage control in distribution systems," in *Proceedings of 18th International Conference and Exhibition on Electricity Distribution*, Turin, Italy, Jun. 2005, pp. 1-6.

[4] R. Seguin, J. Woyak, D. Costyk *et al.* (2006, Jan.). High-penetration PV integration handbook for distribution engineers. [Online]. Available: https://www.osti.gov/biblio/1235905/

[5] R. J. Broderick, J. E. Quiroz, M. J. Reno *et al.* (2013, Jan.). Time series power flow analysis for distribution connected PV generation. [Online]. Available: http://energy.sandia.gov/wp-content/gallery/uploads/SAND_Time-Series-Power-Flow-Analysis-for-Distribution-Connected-PV-Generation.pdf

[6] R. Tonkoski, D. Turcotte, and T. H. M. El-Fouly, "Impact of high PV penetration on voltage profiles in residential neighborhoods," *IEEE Transactions on Sustainable Energy*, vol. 3, no. 3, pp. 518-527, Jul. 2012.

[7] M. A. Cohen and D. S. Callaway, "Effects of distributed PV generation on California's distribution system, Part 1: engineering simulations," *Solar Energy*, vol. 128, pp. 126-138, Apr. 2016.

[8] T. Pfajfar, I. Papic, B. Bletterie *et al.*, "Improving power quality with coordinated voltage control in networks with dispersed generation," in *Proceedings of 9th International Conference on Electrical Power Quality and Utilisation*, Barcelona, Spain, Oct. 2007, pp. 1-6.

[9] A. Keane, L. F. Ochoa, E. Vittal *et al.*, "Enhanced utilization of voltage control resources with distributed generation," *IEEE Transactions on Power Systems*, vol. 26, no. 1, pp. 252-260, Feb. 2011.

[10] K. M. Muttaqi, A. D. T. Le, M. Negnevitsky *et al.*, "A coordinated voltage control approach for coordination of OLTC, voltage regulator, and DG to regulate voltage in a distribution feeder," *IEEE Transactions on Industry Applications*, vol. 51, no. 2, pp. 1239-1248, Apr. 2015.

[11] M. A. Azzouz, M. F. Shaaban, and E. F. El-Saadany, "Real-time optimal voltage regulation for distribution networks incorporating high penetration of PEVs," *IEEE Transactions on Power Systems*, vol. 30, no. 6, pp. 3234-3245, Nov. 2015.

[12] H. Xu, A. D. Domínguez-García, V. V. Veeravalli *et al.*, "Data-driven voltage regulation in radial power distribution systems," *IEEE Transactions on Power Systems*, vol. 35, no. 3, pp. 2133-2143, May 2020.

[13] H. Xu, A. D. Domínguez-García, and P. W. Sauer, "Optimal tap setting of voltage regulation transformers using batch reinforcement learning," *IEEE Transactions on Power Systems*, vol. 35, no. 3, pp. 1990-2001, May 2020.

[14] Q. Yang, G. Wang, A. Sadeghi *et al.*, "Two-timescale voltage control in distribution grids using deep reinforcement learning," *IEEE Transactions on Smart Grid*, vol. 11, no. 3, pp. 2313-2323, May 2020.

[15] T. Abdel-Galil, A. Abu-Elanien, E. El-Saadany *et al.*, "Protection coordination planning with distributed generation," *CETC Varennes*. doi: 10.13140/RG.2.2.35416.80649

[16] Electric Power Research Institute (EPRI). (2017, Mar.). OpenDSS. [Online]. Available: http://smartgrid.epri.com/SimulationTool.aspx

[17] A. S. A. Awad, D. Turcotte, T. H. M. El-Fouly *et al.*, "Impact of distributed generation on the operation of load tap changers in canadian suburban benchmark distribution network," in *Proceedings of IEEE 30th Canadian Conference on Electrical and Computer Engineering (CCECE)*, Windsor, Canada, May 2017, pp. 1-5.

[18] Natural Resources Canada. (2020, Sept.). High-resolution solar radiation datasets. [Online]. Available: http://www.nrcan.gc.ca/energy/renewable-electricity/solar-photovoltaic/18409

[19] Sandia National Laboratories. (2020, Sept.). Wavelet variability model. [Online]. Available: https://pvpmc. sandia. gov/applications/ wavelet-variability-model/

[20] A. Gagné, D. Turcotte, N. Goswamy *et al.*, "High resolution characterisation of solar variability for two sites in Eastern Canada," *Solar Energy*, vol. 137, pp. 46-54, Nov. 2016.

[21] *Terrestrial Photovoltaic (PV) Modules – Design Qualification and Type Approval – Part 2: Test Procedures*. IEC 61215-2, 2016.

[22] Canadian Solar Inc. (2020, Sept.). Data sheet. [Online]. Available: https://www. canadiansolar. com/downloads/datasheets/en/new/Canadian_Solar-Datasheet-_Dymond_CS6K-M-FG_en.pdf

[23] Environment and Climate Change Canada. (2020, Sept.). Historical data. [Online]. Available: http://climate. weather. gc. ca/ historical_data/ search_historic_data_e.html
[24] C. Grigg, P. Wong, P. Albrecht *et al.*, "The IEEE reliability test system-1996: a report prepared by the reliability test system task force of the application of probability methods subcommittee," *IEEE Transactions on Power Systems*, vol. 14, no. 3, pp. 1010-1020, Aug. 1999.
[25] *Preferred Voltage Levels for AC Systems*, CSA Standard C235-83, 2015.
[26] *IEEE Standard for Interconnection and Interoperability of Distributed Energy Resources with Associated Electric Power Systems Interfaces*, IEEE Standard 1547, 2018.

Ahmed S. A. Awad received the B.Sc. and the M.Sc. degrees in electrical engineering from Ain Shams University, Cairo, Egypt, in 2007 and 2010, respectively, and the Ph.D. degree from the Department of Electrical and Computer Engineering, University of Waterloo, Waterloo, Canada, in 2014. From 2007 to 2009, he worked as an Electrical Design Engineer with Dar El-Handasah (Shair and partners) and Allied Consultants Co. in Egypt. He also worked with Siemens Canada Limited from 2014 to 2016. Since 2008, he has been working with the Department of Electrical Power and Machines Engineering, Ain Shams University, Cairo, Egypt. He joined CanmetENERGY, Natural Resources Canada, in 2016, as a Research Engineer, where he is conducting and managing research activities related to active distribution networks and remote microgrids. In 2019, he was appointed as an Adjunct Assistant Professor at the Electrical and Computer Engineering Department, University of Windsor, Windsor, Canada. He is currently an Editor for the IEEE Transactions on Sustainable Energy, and a Registered Professional Engineer in the Province of Ontario, Canada. His research interests include application of energy storage in smart grids, integration of renewable energy resources, electricity market equilibrium, as well as operation and control of distribution systems.

Dave Turcotte received the B.A.Sc. degree in electrical engineering in 1996 from Université de Sherbrooke, Quebec, Canada. He joined the CanmetENERGY Centre in Varennes, Canada, in January 1997, where he has been working on various projects related to photovoltaics, power conversion, and grid integration of renewables. He is actively involved in product and interconnection standards in Canada and abroad. His research interests include advising, planning, and coordinating R&D activities with various members of the Renewable Energy Integration team to ensure cohesion, adequacy and impact in the Canadian context.

Tarek H. M. El-Fouly received the B.Sc. and M.Sc. degrees in electrical engineering from Ain Shams University, Cairo, Egypt, in 1996 and 2002, respectively, and the Ph.D. degree in electrical engineering from the University of Waterloo, Waterloo, Canada, in 2008. He joined CanmetENERGY in 2008 as a Transmission and Distribution Research Engineer and was promoted to Smart Microgrids Research Manager in 2014. From 2010 to 2017, he was appointed as an Adjunct Assistant Professor at the Electrical and Computer Engineering Department, University of Waterloo. In January 2015, he joined Khalifa University, Abu Dhabi, UAE, as an Assistant Professor at the Electrical Engineering and Computer Science Department and was promoted to Associate Professor in July 2019. He is serving as an Associate Editor for IEEE Access and IET Renewable Power Generation. He research interests include smart grids, microgrids, high penetration of renewable energy resources, and integration of electrical energy storage systems.